Earthline Journal of Chemical Sciences
E-ISSN: 2581-9003; CODEN: EJCSB4
Volume 12, Number 3, 2025, Pages 291-310
https://doi.org/10.34198/ejcs.12325.291310

DFT treatment of some isomers of griseofulvin

Lemi Türker

Department of Chemistry, Middle East Technical University, Üniversiteler, Eskişehir Yolu No: 1, 06800 Çankaya/Ankara, Turkey
e-mail: lturker@gmail.com; lturker@metu.edu.tr

Abstract

Griseofulvin is an antifungal agent and is used to treat skin infections, fungal infections of the scalp, fingernails, and toenails etc. In the present study, various stereo/regio isomers of griseofulvin have been investigated within the constraints of density functional theory (DFT) at the levels of B3LYP/6-31+G(d,p) and partly B3LYP/6-31++G(d,p). All the isomers presently considered (in vacuum conditions) have exothermic heat of formation values and also possess favorable Gibbs free energy of formation values. In addition to that they are electronically stable structures. Various quantum chemical data have been collected and discussed including the HOMO, LUMO energies, and IR and UV-VIS spectra.

1. Introduction

Griseofulvin ($C_{17}H_{17}ClO_6$) ((2S,6′R)-7-chloro-4,6-dimethoxybenzofuran-3-one-2-spiro-1′-(2′-methoxy-6′-methylcyclohex-2′-en4′-one) is formed by fungi of the genus of *Penicillium* (*P. urticae*, *P. nigricans*, *P. raistrichi*, etc.). Griseofulvin is used to treat skin infections such as jock itch, athlete's foot, and ringworm and fungal infections of the scalp, fingernails, and toenails. Griseofulvin is produced industrially by submerged cultivation of *Penicillium urticae* in a medium containing corn-steep liquor, lactose, KH_2PO_4 and KCl. The synthesis is stimulated by ammonium tartarate [1]. In Soviet Union *Penicillium nigricans* was used for griseofulvin. This mold does not produce a very toxic substance called ratulin [1]. Griseofulvin is effective against various forms of mycoses of the smooth skin, the hair and nails. However of the different restrictions for using griseofulvin mentioned should be malignant tumors, acute disease of the liver, pregnancy and purphyria, leucopenia etc. [2,3].

The history of griseofulvin has been surveyed by Petersen and coworkers [4]. Initial research was aimed at the structural elucidation of the fungal metabolite, and later emphasis was on synthesizing analogs for biological investigation of the antifungal properties, both by semi synthesis from griseofulvin and by de novo synthesis [4].

The chemistry of griseofulvin and analogs has been reviewed making an updated and comprehensive overview of the literature [5, 6]. Note that griseofulvin was initially isolated from *Penicillium griseofulvum* in 1939 by Oxford et al., [7].

Some analogous metabolites dechlorogriseofulvin and 7-bromo-7-dechloro-griseofulvin were later isolated by MacMillan [8]. Griseofulvin has been the subject of very many recent research articles [9-20]. Besides the numerous number of articles about its biological and medicinal usage/properties etc., there exist others. Such as, metal (II) and metal (III) coordination compounds of griseofulvin drug were synthesized by Mahmoud et al.,

Received: June 20, 2025; Accepted: July 15, 2025; Published: July 20, 2025

Keywords and phrases: griseofulvin, fungi, griseofulvin isomers, DFT calculations, spectra.

[17] and besides other investigations, density functional theory (DFT) calculations were employed to understand and estimate the contribution of each interaction in the formation of the assembly using several theoretical models [17]. Thermo chemical analysis of the dissolution process of griseofulvin was studied by Knoblauch and Zimmermann [18]. Coformer substitution in cocrystallization involving griseofulvin and phenol derivatives has been investigated by Lasser and Braun [19]. Hydrotropic action of hydrotrope sodium cumene sulfonate on the solubility of drug griseofulvin was investigated by Das and Paul [20]. Griseofulvin is still remaining as a hot topic in the literature.

2. Method of Calculations

In the present study, all the initial optimizations of the structures leading to energy minima have been achieved by using MM2 method first which is then followed by semi empirical PM3 self consistent fields molecular orbital method [21-23]. Afterwards, the structure optimizations have been achieved within the framework of Hartree-Fock and finally by using density functional theory (DFT) at the levels of B3LYP/6-31+G(d,p) and partly B3LYP/6-31++G(d,p) [24,25]. Note that the exchange term of B3LYP consists of hybrid Hartree-Fock and local spin density (LSD) exchange functions with Becke's gradient correlation to LSD exchange [26]. The correlation term of B3LYP consists of the Vosko, Wilk, Nusair (VWN3) local correlation functional [27] and Lee, Yang, Parr (LYP) correlation correction functional [28]. In the present study, the normal mode analysis for each structure yielded no imaginary frequencies for the $3N–6$ vibrational degrees of freedom, where N is the number of atoms in the system. This search has indicated that the structure of each molecule considered corresponds to at least a local minimum on the potential energy surface. Furthermore, all the bond lengths have been thoroughly searched in order to find out whether any bond cleavage occurred or not during the geometry optimization process. All these computations were performed by using SPARTAN 06 program [29].

3. Results and Discussion

The present treatise concentrates on some stereo and/or regio isomers of griseofulvin within the realm of density functional theory. It is worth remembering that all the odd numbered structures have *exo* whereas even numbered ones have *endo* stereochemistry.

In the present study, the terms *exo* and *endo* are defined according to the chirality of methyl bearing carbon atom (in the six-membered ring) whether it is R or S (*exo* and *endo*, respectively). Figure 1 shows the optimized structure of griseofulvin at the level of B3LYP/6-31++G(d,p). Note that the basis sets presently used have diffuse functions and are very popular for quantitative results for organic molecules.

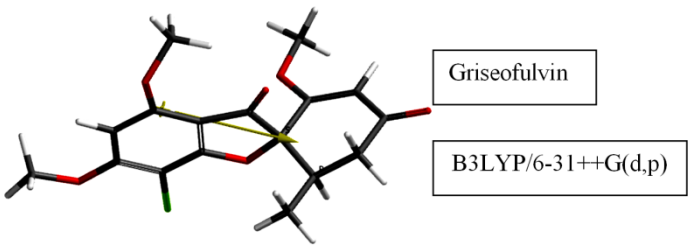

Figure 1. Optimized structure of griseofulvin.

Figure 2 shows the optimized structures of two stereoisomers of griseofulvin obtained at the level of 6-31+G(d). Note that the chirality of the spiro center is S in all the cases. Also note that in the *endo* case,

conformation of one of the methoxy groups attached to the aromatic ring is different from the respective one in the *exo* case.

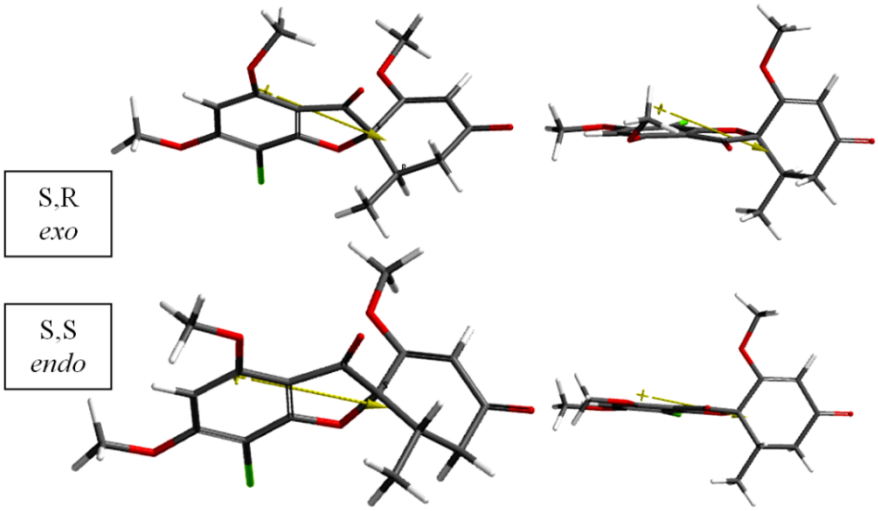

Figure 2. Different views of the optimized structures of two stereoisomers of griseofulvin (6-31+G(d), the chirality of the spiro center is S).

Calculated bond lengths of the *exo* and *endo* isomers of griseofulvin are depicted in Figure 3. The data of the table indicate that some respective bond lengths are different in the *exo* and *endo* isomers.

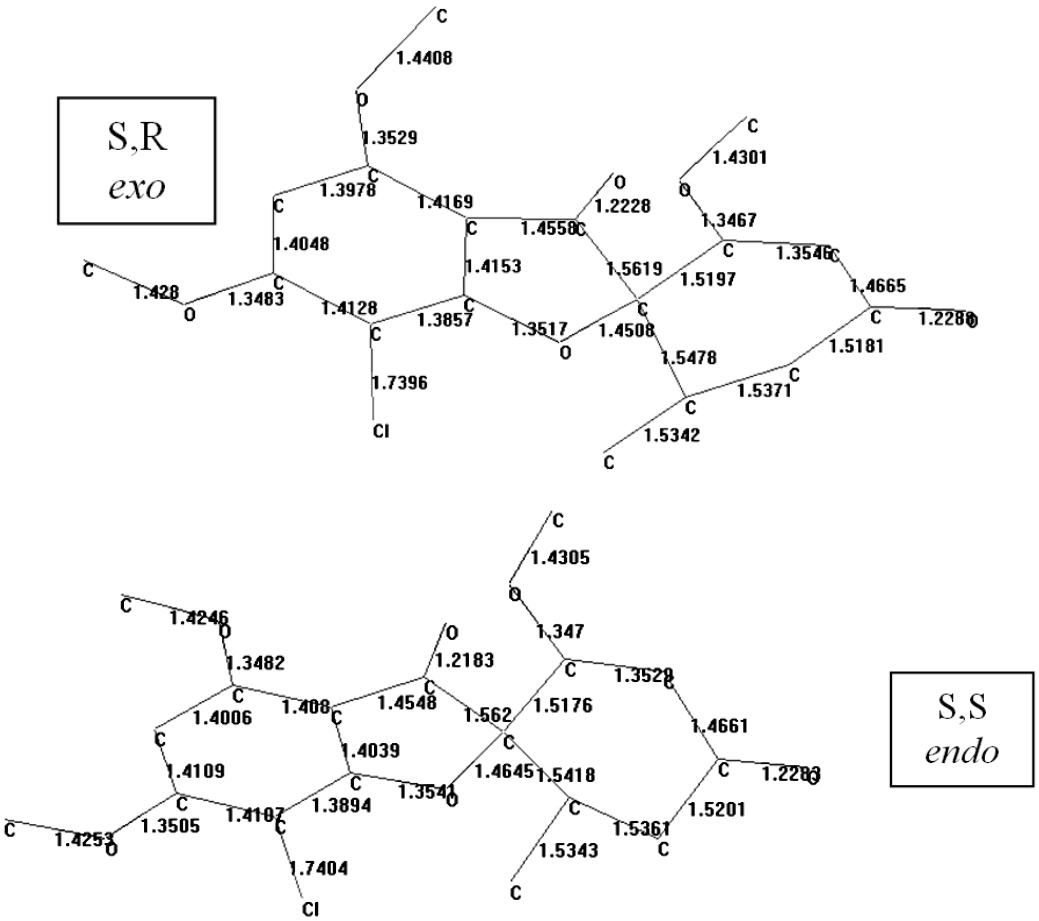

Figure 3. Calculated bond lengths of the *exo* and *endo* isomers of griseofulvin (hydrogens omitted).

The calculated IR spectra of the *exo* and *endo* isomers of griseofulvin are shown in Figure 4. Various ring deformations take place in between 1759-1593 cm^{-1} in the *exo* and 1783-1544 cm^{-1} in the *endo* isomer. In the first case, the stretching occurring at 1759 cm^{-1} belongs the five-membered ketone carbonyl which is followed by six-membered ketone carbonyl at 1735 cm^{-1}. The huge peak at 1661 cm^{-1} is C=C stretch of the 6-membered ring. The skeletal breathing of aromatic ring is at 1649 cm^{-1}, 1593 cm^{-1}.

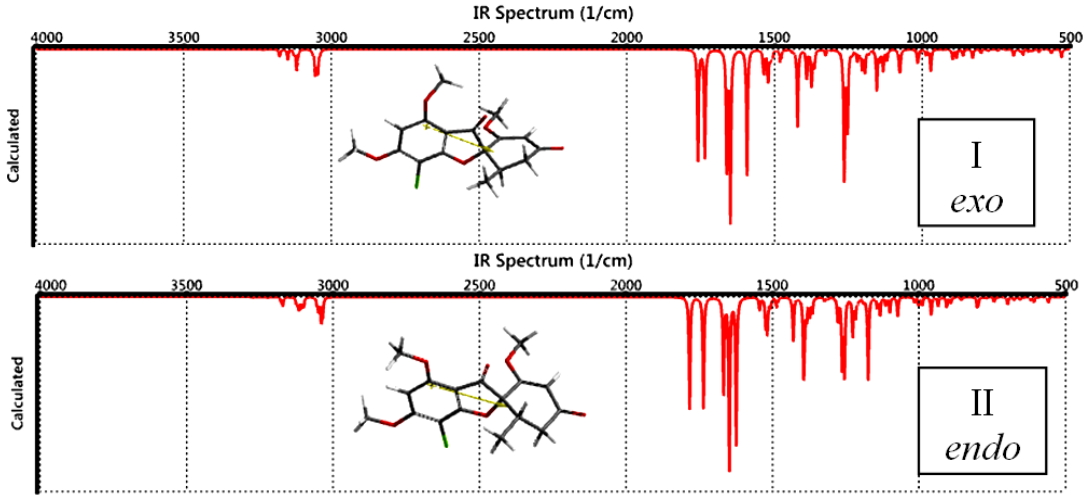

Figure 4. The calculated IR spectra of *exo* and *endo* isomers of griseofulvins.

In the *endo* isomer carbonyl of 5-membered ring occurs at 1783 cm^{-1} whereas the carbonyl of the 6-membered ring is at 1736 cm^{-1}. The C=C stretch of the 6-membered ring happens at 1667 cm^{-1}. Various ring stretchings take place at 1624-1647 cm^{-1}.

The calculated UV-VIS spectra (time dependent) of the *exo* and *endo* isomers of griseofulvin are shown in Figure 5. As seen in the figure, they both absorb in the ultraviolet region of the spectrum because in the structures no extended-conjugation having chromophor/auxochrome exist, except the aromatic ring, to shift the absorption to longer wavelengths.

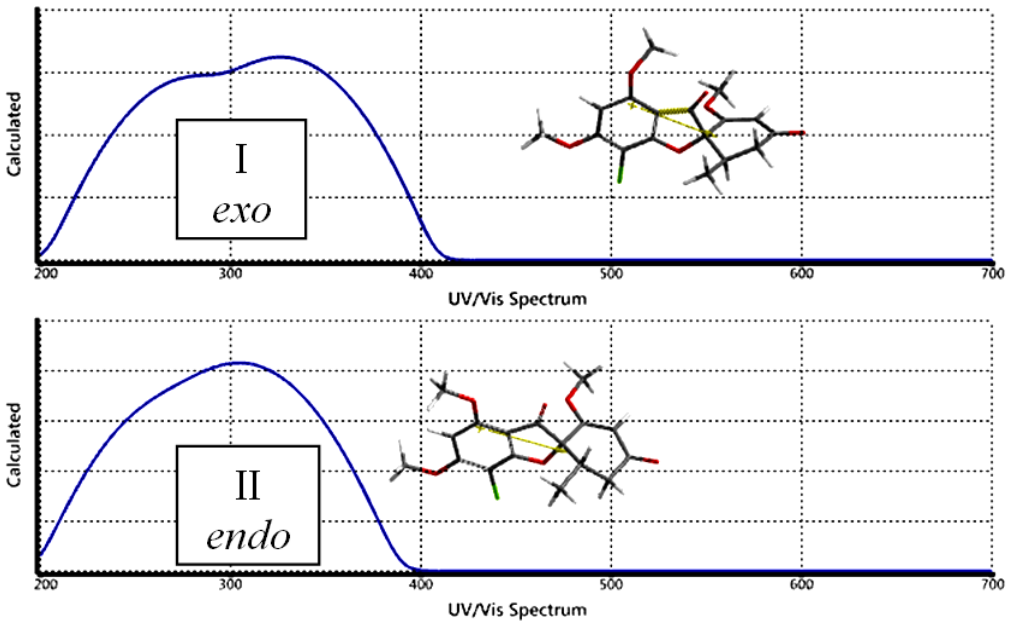

Figure 5. The calculated UV-VIS spectra of *exo* and *endo* isomers of griseofulvin.

Figure 6 shows the optimized structures of some griseofulvin isomers considered which are stereo and/or regio isomers of each other.

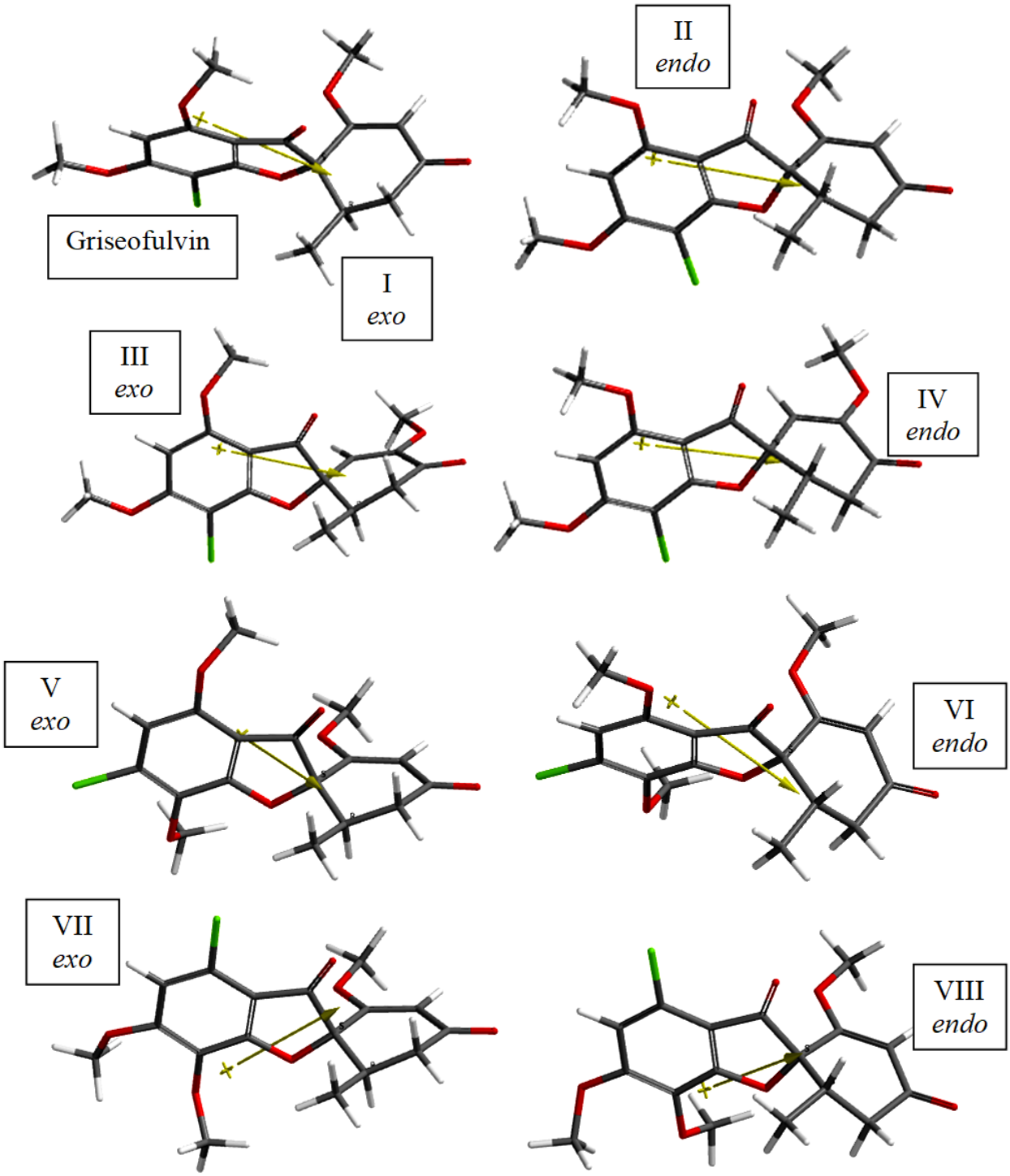

Figure 6. Optimized structures of some griseofulvin isomers considered.

Table 1 displays some thermo chemical properties of the griseofulvin isomers considered. The data reveal that the standard heat of formation (Hº) values of all the species are exothermic, and they are favored according to their Gº (Gibbs free energy of formation) values. The algebraic order of Hº and Gº values for isomeric tautomers are (B3LYP/6-31+G(d) level) II<I<VI<V<IV<VIII<III<VII and II<I<VI<IV<V<VIII<III<VII, respectively. Both of the orders are almost the same except the orders of IV and V.

The heat of formation values of some griseofulvin isomers at different level of calculations are listed in Table 2. The orders of PM3//B3LYP/6-31+G(d) calculations is II<IV<VI<I<III<VIII<VII<V, whereas T1 calculations give the order of II<I<VI<V<VIII<VII<III<IV. Note that T1 is a thermo chemical recipe which has been developed to closely reproduce heat of formation calculated from G3(MP2). Although the presented orders of heat of formations differ from methodologies of one to other, they all yield exothermic values. The other common point to emphasize is that the *endo* form is more exothermic than the *exo* isomer.

Table 1. Some thermo chemical properties of the griseofulvin isomers considered.

Isomers	Chirality	H^o	S^o (J/mol^o)	G^o
I (Griseofulvin)				
(B3LYP/6-31++G(d,p))	S,R	-4120144.876	582.64	-4120318.581
I (Griseofulvin)	S,R	-4120080.472	582.14	-4120254.019
II (Griseofulvin)	S,S	-4120084.673	582.41	-4120258.299
III	S,R	-4120058.995	581.91	-4120232.490
IV	S,S	-4120061.017	582.84	-4120234.801
V	S,R	-4120061.490	580.88	-4120234.696
VI	S,S	-4120070.101	582.73	-4120243.832
VII	S,R	-4120057.262	582.57	-4120230.941
VIII	S,S	-4120060.597	583.68	-4120234.643

Energies in kJ/mol. Chirality of the spiro center is S in all the cases. Otherwise stated B3LYP/6-31+G(d) level of calculations.

Table 2. The heat of formation values of some griseofulvin isomers.

Isomers	Stereo form*	PM3//B3LYP/6-31+G(d)	T1
I (Griseofulvin)	*exo*	-717.128	-800.43
II (Griseofulvin)	*endo*	-733.375	-801.62
III	*exo*	-714.816	-778.62
IV	*endo*	-728.798	-777.40
V	*exo*	-704.251	-789.77
VI	*endo*	-720.477	-794.19
VII	*exo*	-706.199	-785.56
VIII	*endo*	-707.811	-788.00

Energies in kJ/mol. *Stereo form of 6'-methyl group attached to 6-membered ring.

Table 3 displays some energies of the griseofulvin isomers considered where E, ZPE and E_C stand for the total electronic energy, zero point vibrational energy and the corrected total electronic energy, respectively. According to the data, they are all electronically stable structures. The stability order for isomeric species

(B3LYP/6-31+G(d) level) is II>I>VI>V>IV>VIII>III>VII. In each case, the *endo* isomer is more exothermic, more favorable additionally electronically more stable compared to the respective *exo* isomer.

Table 3. Some energies of the griseofulvin isomers considered.

Isomers	E	ZPE	E_C
I (Griseofulvin)			
B3LYP/6-31++G(d,p) (*exo*)	-4120989.737	829.50	-4120160.23
I (Griseofulvin) (*exo*)	-4120928.28	832.54	-4120095.74
II (Griseofulvin) (*endo*)	-4120933.26	833.32	-4120099.94
III (*exo*)	-4120906.45	832.15	-4120074.30
IV (*endo*)	-4120909.06	832.75	-4120076.31
V (*exo*)	-4120908.70	831.87	-4120076.83
VI (*endo*)	-4120916.52	831.00	-4120085.52
VII (*exo*)	-4120903.62	830.93	-4120072.69
VIII (*endo*)	-4120906.61	830.52	-4120076.09

Energies in kJ/mol. Otherwise stated B3LYP/6-31+G(d) level of calculations.

The aqueous and solvation energies of some of the griseofulvin isomers considered are shown in Table 4. The algebraic order of aqueous and solvation energy values are II<I<VI<IV<V<VIII<III<VII and II<IV<VI<I<VII<VIII<III<V, respectively. Stereo and regio isomerism of the groups, thus their hydrogen bond formation possibilities and their stabilities, etc., dictate the orders obtained presently. The solvation energies were calculated by adopting SM5.4/A model [29]. Note that they are all exothermic in character. The algebraic order of E_{aq} and E_{solv} values are II<I<VI<IV<V<VIII<III<VII and II<IV<VI<I<VII<VIII<III<V, respectively. The responsible factors in establishing these orders might be orientation of the groups, their charge distributions, charge-dipole and/or dipole-dipole interactions within the molecule itself and the solvent, etc.

Table 4. The aqueous and solvation energies of some of the griseofulvin isomers considered.

Isomers	E_{aq} (kJ/mol)	E_{solv}
I (Griseofulvin) (*exo*)	-4120961.64	-33.356
II (Griseofulvin) (*endo*)	-4120975.28	-42.020
III (*exo*)	-4120935.70	-29.246
IV (*endo*)	-4120946.49	-37.438
V (*exo*)	-4120937.84	-29.143
VI (*endo*)	-4120952.28	-35.762
VII (*exo*)	-4120935.63	-32.013
VIII (*endo*)	-4120936.97	-30.363

Energies in kJ/mol. B3LYP/6-31+G(d) level of calculations. Solvation energy by SM5.4/A model.

Figure 7 stands for the electrostatic potential (ESP) charges on atoms of griseofulvin (B3LYP/6-31++G(d,p)).

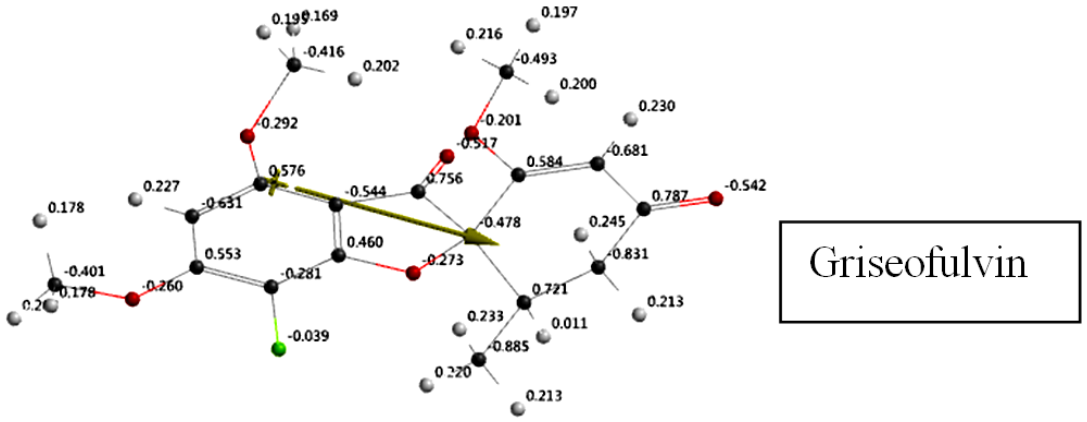

Figure 7. ESP charges on atoms of griseofulvin (B3LYP/6-31++G(d,p)).

The ESP charges on atoms of some griseofulvin isomers (B3LYP/6-31+G(d) level) are shown in Figure 8.

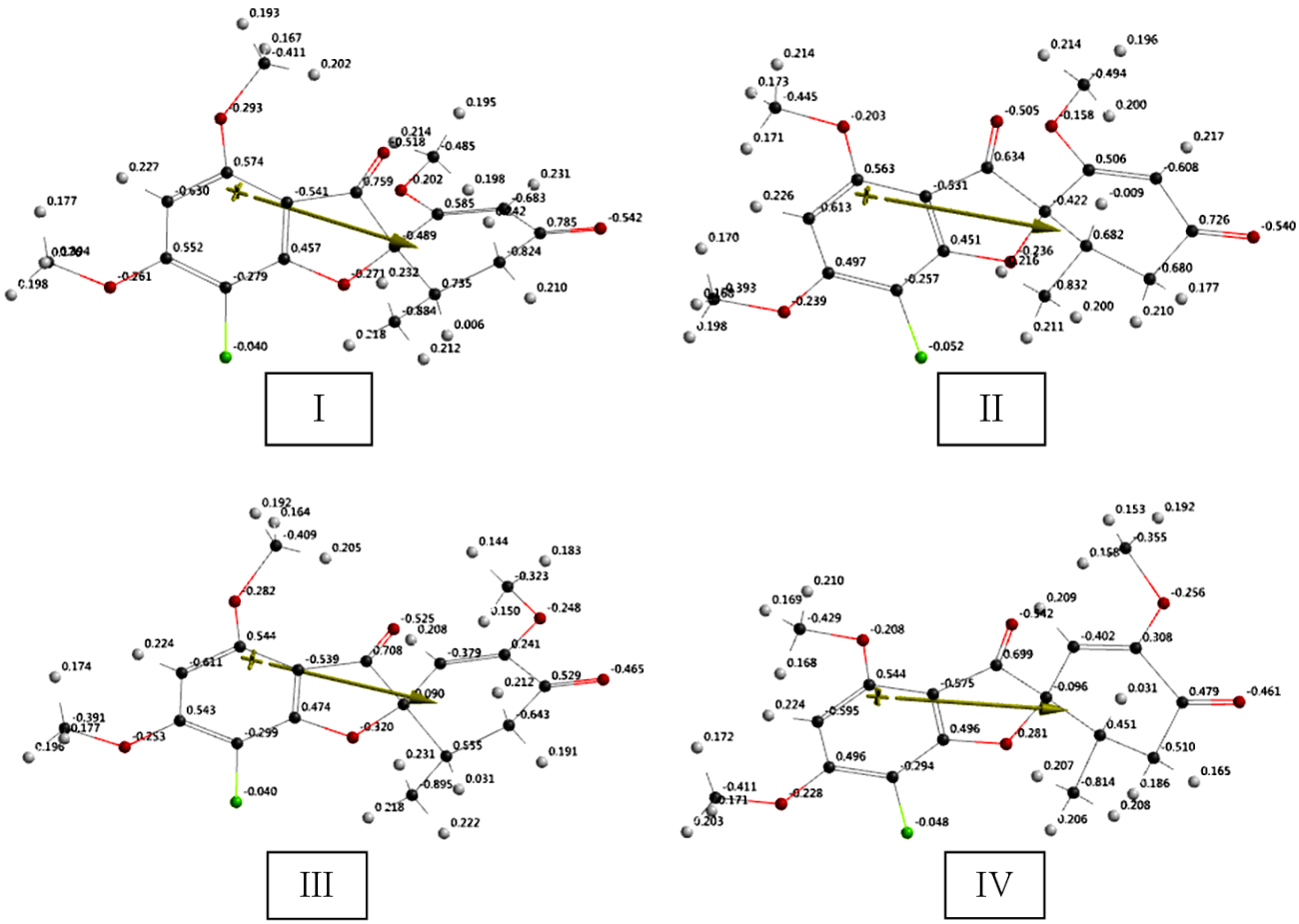

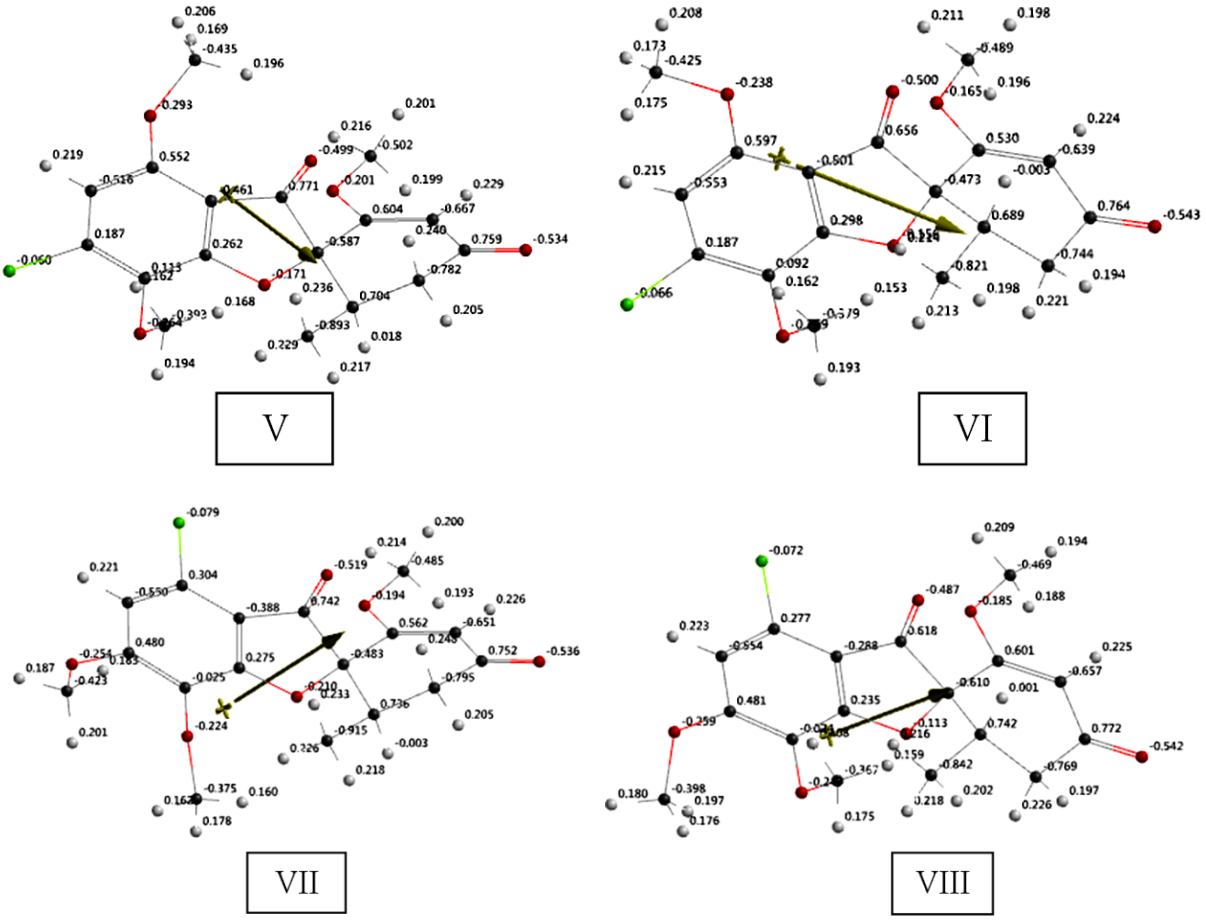

Figure 8. ESP charges on atoms of some griseofulvin isomers (B3LYP/6-31+G(d)).

Figure 9 shows the ESP maps of some griseofulvin isomers considered where negative potential regions reside on red/reddish and positive ones on blue/bluish parts of the maps. Notice the effect of regio isomerism on the maps, e.g., structures II and III have the methoxy group on different positions of C=C bond and red/orange regions differ.

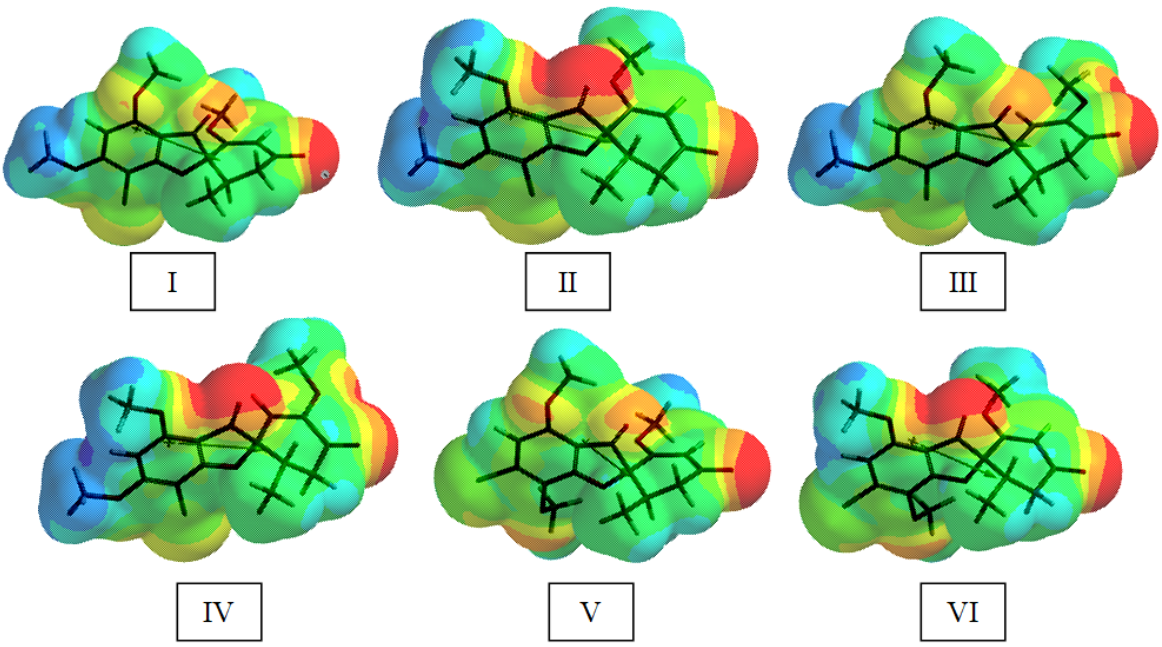

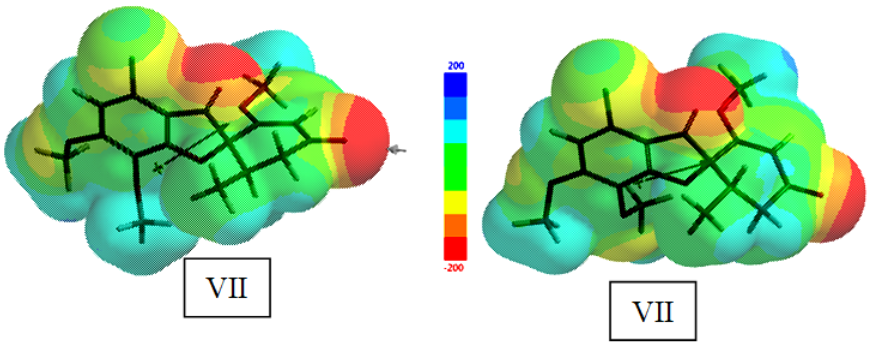

Figure 9. ESP maps of some griseofulvin isomers considered.

Some of the molecular orbital energy levels of the isomers considered are shown in Figure 10. Note that densely spaced inner lying orbitals are related to thermal stability.

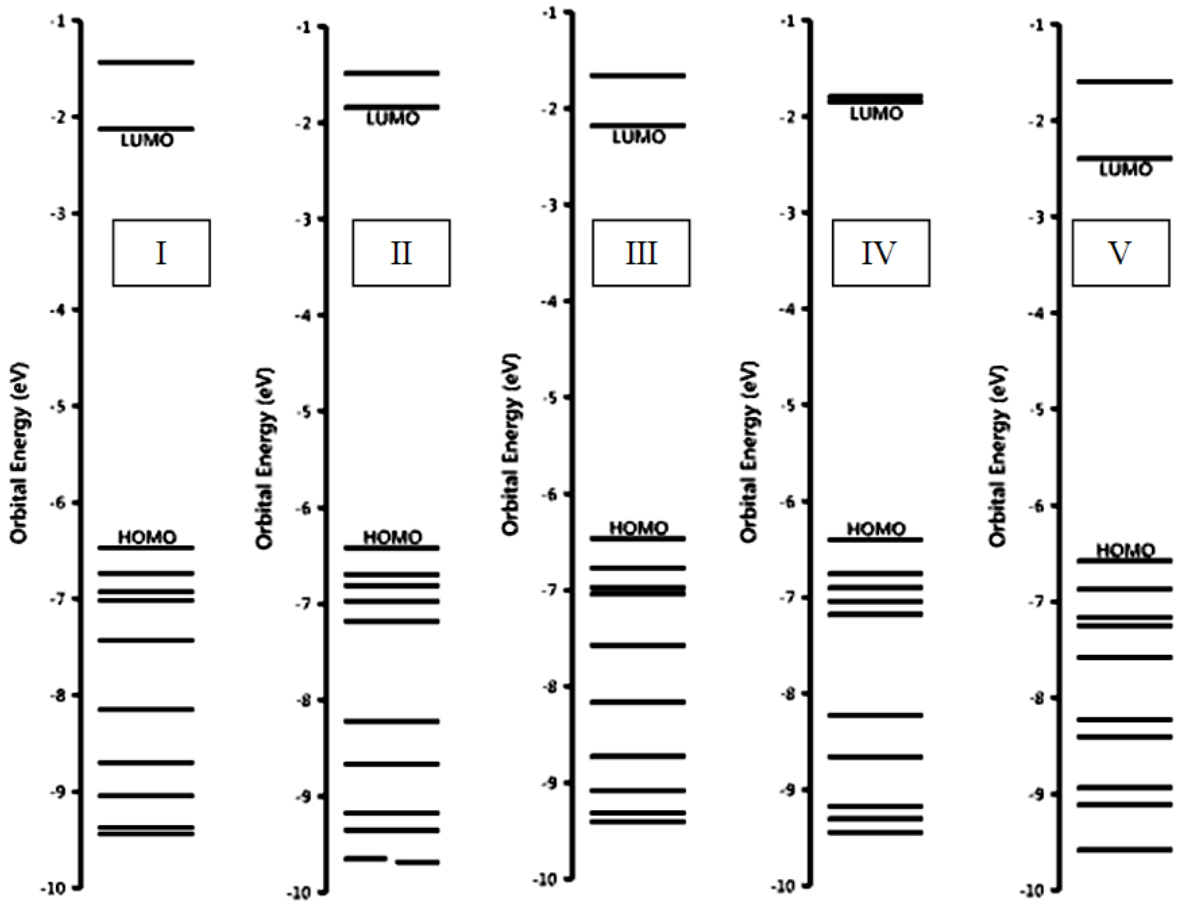

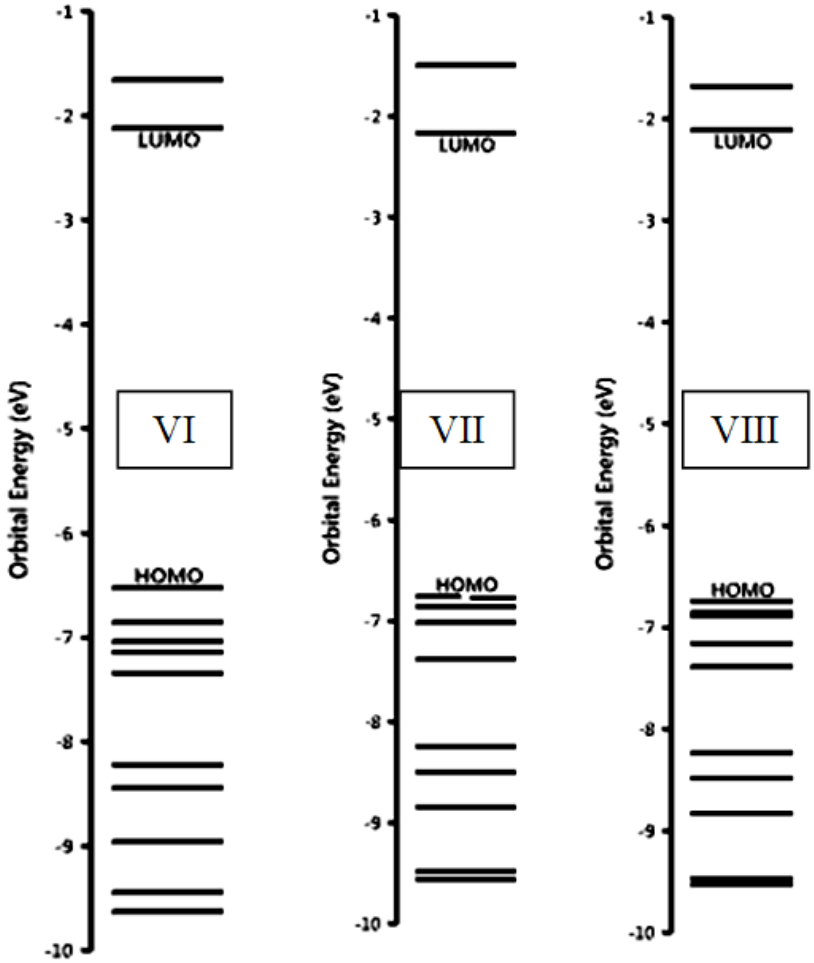

Figure 10. Some of the molecular orbital energy levels of the isomers considered.

Table 5 includes the HOMO, LUMO energies and interfrontier molecular orbital energy gap values (Δε) values of the griseofulvin isomers considered. Note that $\Delta\varepsilon = \varepsilon_{LUMO}-\varepsilon_{HOMO}$. It is worth mentioning that in each case the HOMO energy of the *exo* form is lower (algebraic) than the respective *endo* isomer. The same trend is also true for the LUMO energies which dictate the order of Δε values.

Table 5. The HOMO, LUMO energies and Δε values of the griseofulvin isomers considered.

Isomers	HOMO	LUMO	Δε
Griseofulvin B3LYP/6-31++G(d,p) (exo)	-624.32	-205.07	419.25
I (Griseofulvin) (*exo*)	-624.39	-204.79	419.60
II (Griseofulvin) (*endo*)	-619.19	-177.08	442.11
III *exo*)	-623.91	-209.92	413.99
IV (*endo*)	-617.71	-178.41	439.30
V (*exo*)	-634.56	-230.48	404.08
VI (*endo*)	-629.16	-204.03	425.13
VII (*exo*)	-651.50	-208.97	442.53
VIII (*endo*)	-650.53	-203.28	447.25

Energies in kJ/mol. Otherwise stated B3LYP/6-31+G(d) level of calculations.

Figure 11 shows the HOMO and LUMO patterns of the isomers considered. As seen in the figure, the frontier molecular orbitals, HOMO and LUMO, generally have pi symmetry. The HOMO is mainly constructed by the contribution of the aromatic ring. The 6-membered alicyclic ring either contributes nothing to the HOMO or very little with the exception of III. As for the LUMO, the main contributions are from the aromatic moiety and the 5-membered ring. The 6-membered ring supplies comparatively little.

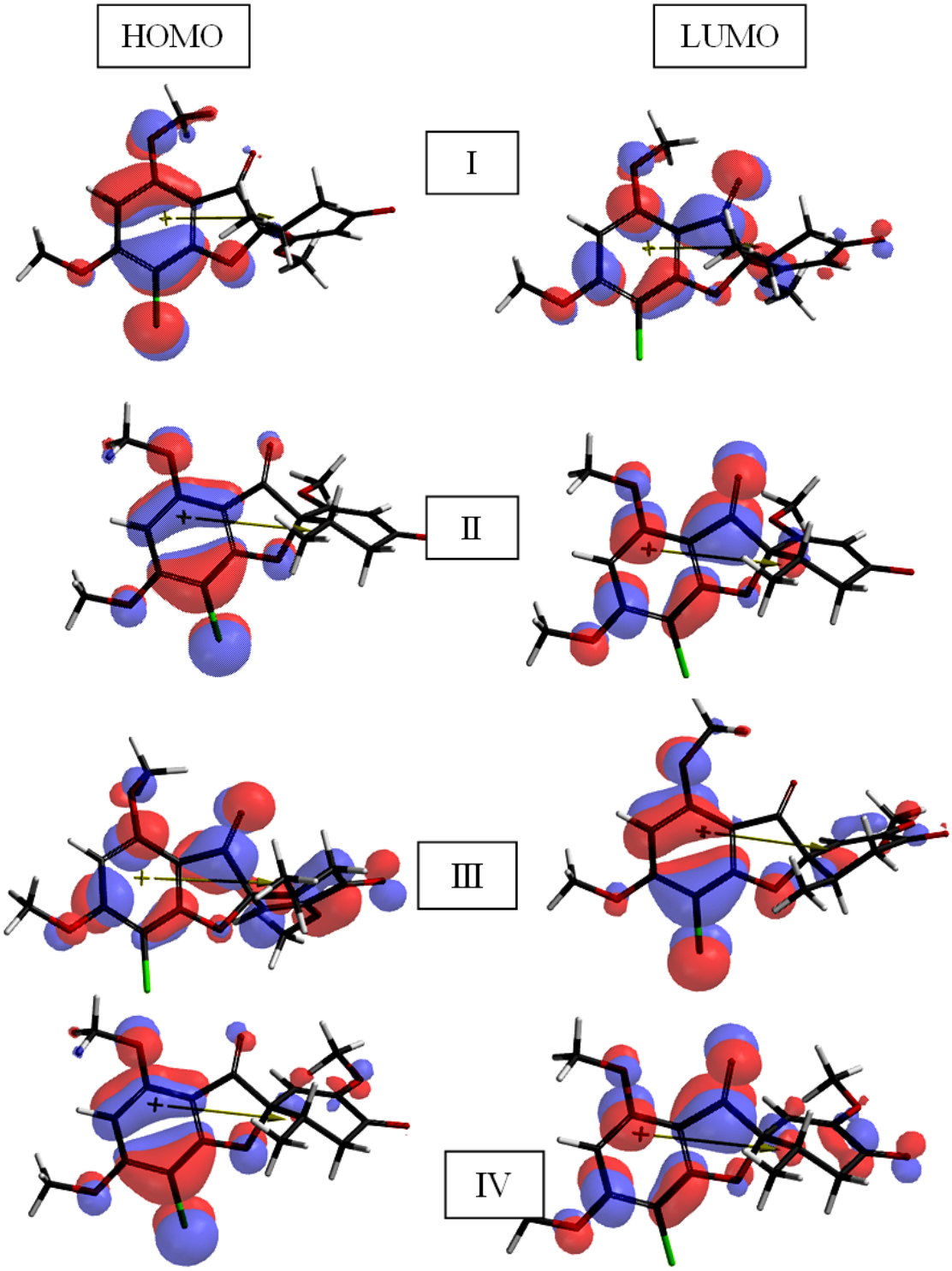

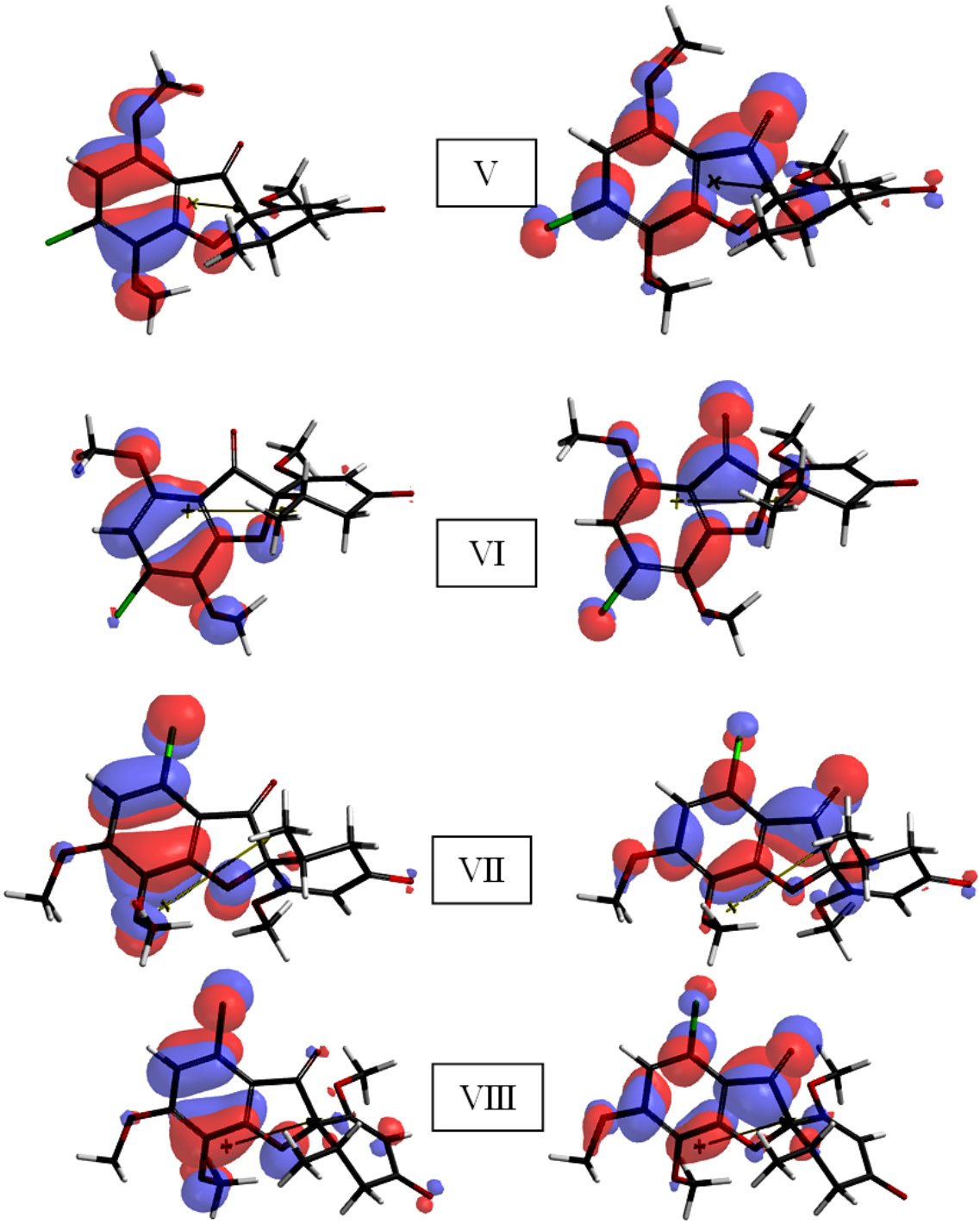

Figure 11. The HOMO and LUMO patterns of the isomers considered.

Some properties of the griseofulvin isomers considered are listed in Table 6. As seen in the table some of the properties listed are highly structure dependent. For instance the dipole moment values as well as their directions (see Figures 2 and 6) vary. The order of dipole moments is II>IV>VII>I>III>VIII>VI>V. In general, the *endo* structures possess greater dipole moment values compared to their respective *exo* isomer with the exception of VII and VIII. Note that they have the same regio chemistry but different stereo chemistry. Since the resultant dipole moment of a molecule is the vectorial sum of the bond dipole moments, which are some intricate function of the geometry and local charges the outcome mentioned above is not unexpected.

Table 6. Some properties of the griseofulvin isomers considered.

Isomers	Dipole (debye)	Polarizability	PSA (Å²)	Area (Å²)	Volume (Å³)
Griseofulvin (B3LYP/6-31++G(d,p)) (*exo*)	6.55	66.78	54.023	342.88	325.91
I (Griseofulvin) (*exo*)	6.56	66.79	54.037	342.98	325.96
II (Griseofulvin) (*endo*)	8.88	66.74	55.841	346.71	326.07
III (*exo*)	6.49	66.81	54.300	343.50	326.09
IV (*endo*)	8.78	66.77	56.731	347.55	326.32
V (*exo*)	4.61	66.88	54.375	344.42	326.63
VI (*endo*)	5.28	66.83	55.987	347.99	326.69
VII (*exo*)	7.29	66.81	54.257	346.78	326.93
VIII (*endo*)	5.75	66.80	54.323	347.43	326.89

Energies in kJ/mol. Polarizabilities in 10^{-30} m^3 units. Otherwise stated, B3LYP/6-31+G(d) level of calculations. Log P values in all cases: -1.78.

It is worth mentioning that the polar surface area (PSA) is defined as the amount of molecular surface area arising from polar atoms (N,O) together with their attached hydrogen atoms. Although these compounds are isomeric, their PSA values differ from each other, meaning that the same kind of atoms might be influenced by electronic factors differently at different positions.

As for the log P values, note that a negative value for log P means the compound has a higher affinity for the aqueous phase (it is more hydrophilic); when log P = 0 the compound is equally partitioned between the lipid and aqueous phases; whereas a positive value for log P denotes a higher concentration in the lipid phase (i.e., the compound is more lipophilic). In the present case, Log P values of all the structures are -1.78, thus they have at least comparable affinity/tendency for the aqueous phase. Consequently, any bioactivity differences between them should be due to stereo and/or regio isomerism they possess. Note that logP is an important parameter/ variable in various correlation/regression attempts of structure-activity relationships in drug design studies.

Figure 12 shows the exposed areas [29] of atoms of *exo* and *endo* griseofulvins. Note that structures in the figure are stereo/regio isomers however the exposed surface areas of respective atoms are quite different (compare the values for the aromatic ring). Because they are affected by various factors such as electron distribution in the molecule, position of the substituents etc. They are effective in directing the interactions between the molecules such as solute-solvent interactions, etc.

Figure 13 shows the local ionization potential maps of the isomers considered where conventionally red/reddish regions (if any exists) on the density surface indicate areas from which electron removal is relatively easy, meaning that they are subject to electrophilic attack. It is worth remembering that the local ionization potential map is a graph of the value of the local ionization potential on an isodensity surface corresponding to a van der Waals surface.

Note that the local ionization potential maps of these isomeric species are highly structure dependent. Even the present stereo chemistry affects the maps. For instance, in the case of isomers I and II; III and IV; V and VI; (they are *exo* and *endo* stereoisomers, respectively).

Moreover, the conformation of the methoxy groups in the *exo* and *endo* species are different. All these conformational and stereo/regio isomeric variations make the maps, (true for LUMO maps, see Figure 14) quite different from each other.

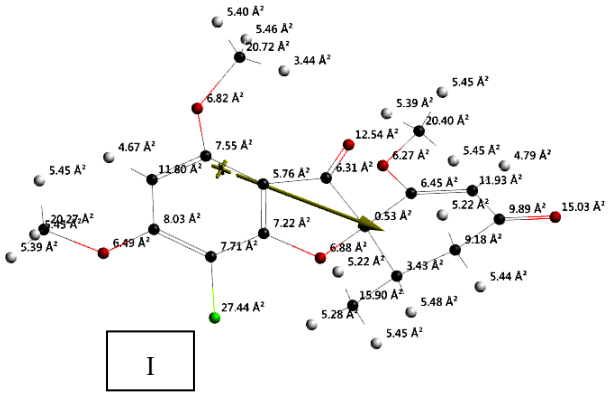

I

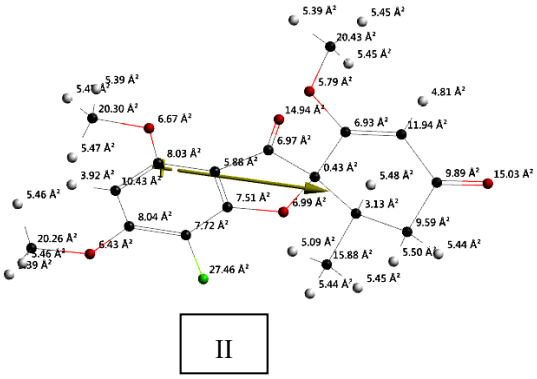

II

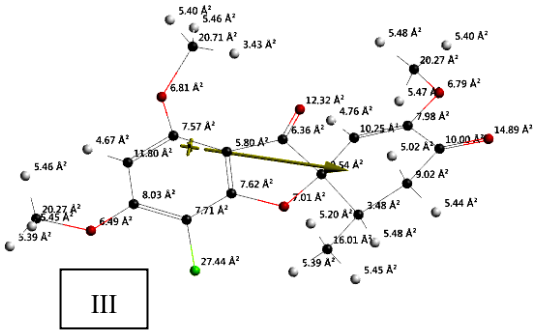

III

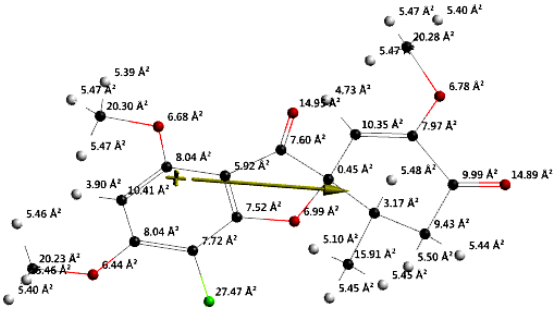

IV

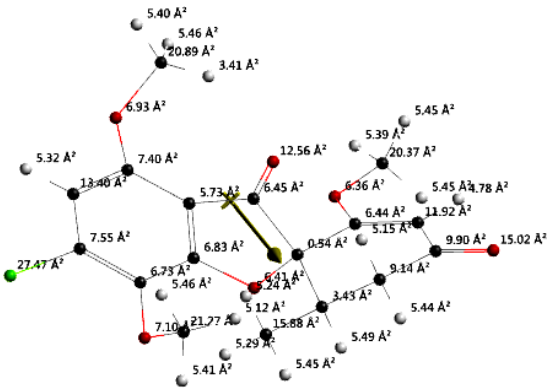

V

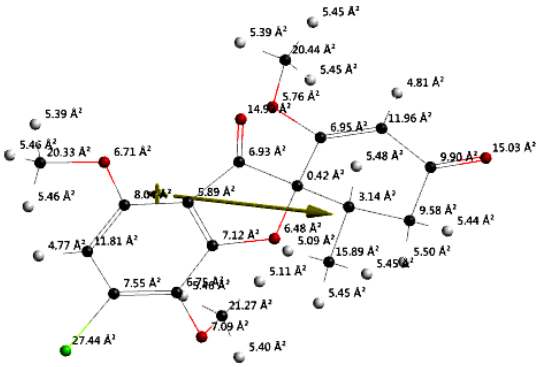

VI

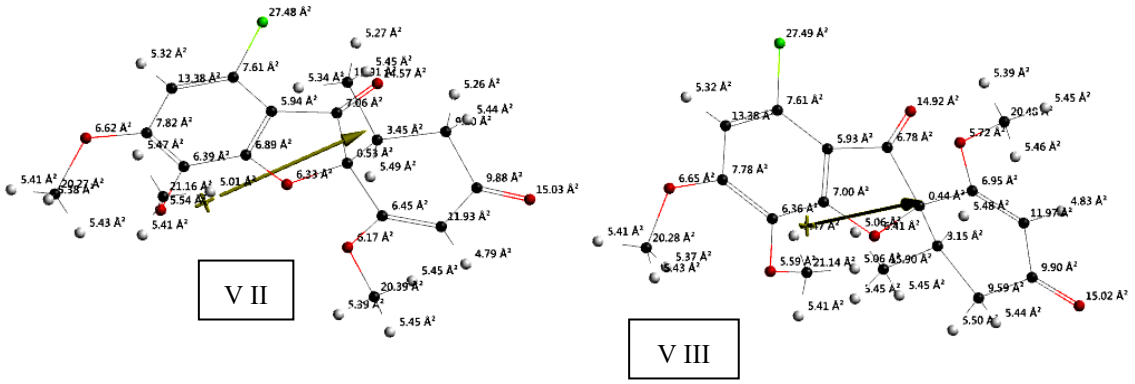

Figure 12. The exposed areas of atoms in *exo* and *endo* griseofulvin species.

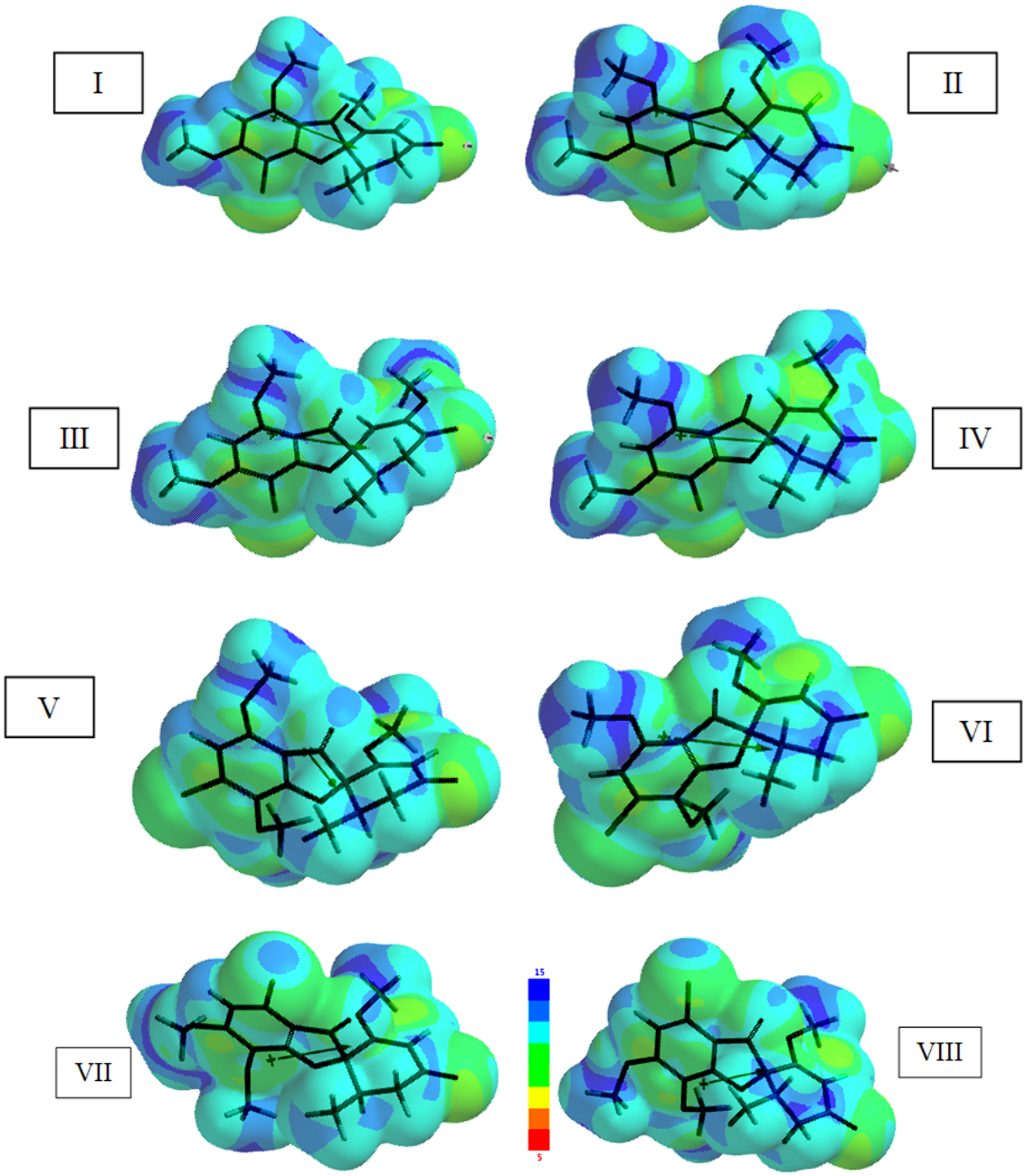

Figure 13. The local ionization potential maps of the isomers considered.

The LUMO maps of the isomeric griseofulvin species considered are shown in Figure 14. Note that a LUMO map displays the absolute value of the LUMO on the electron density surface. The blue color (if any exists) stands for the maximum value of the LUMO and the red colored region, associates with the minimum value. Note that the LUMO and NEXTLUMO are the major orbitals directing the molecule towards of the attack of nucleophiles [29]. Positions where the greatest LUMO coefficient exists is the most vulnerable site in nucleophilic reactions.

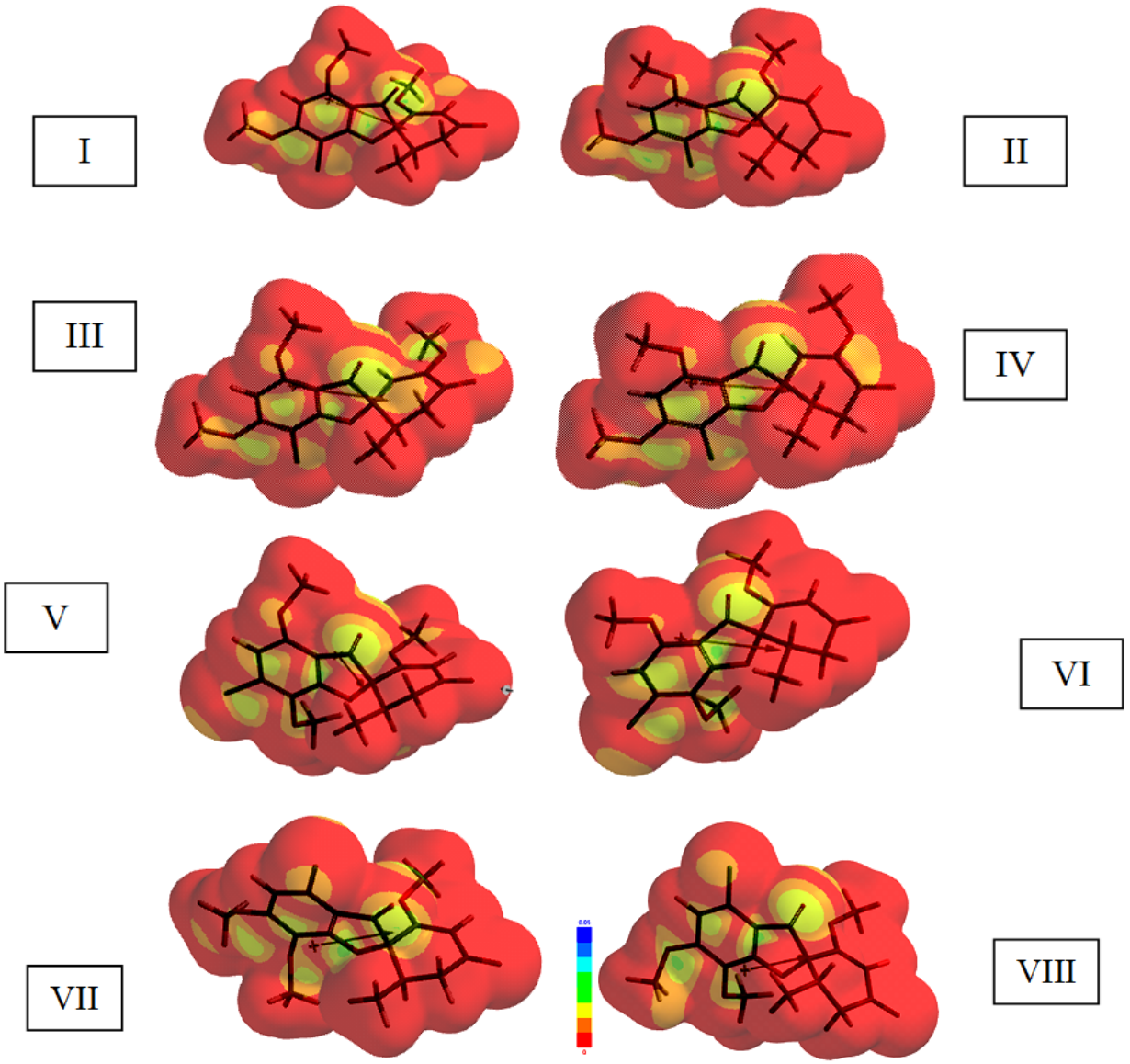

Figure 14. The LUMO maps of the isomeric species considered.

The time dependent density functional (TDDFT) spectra of the griseofulvin isomers considered yielded λ_{max} values which are tabulated in Table 7. The table lists numbers of the structures and their stereo chemistry labels. Due to the lack of extended conjugation in the structures, isomers absorb in the ultraviolet region. Note that the methoxy groups and chlorine atom attached to the aromatic ring exert their inductive and mesomeric effects in some structures fortifying and in some structure diminishing each others effects. All these factors are structure dependent. Also note that the presence of the spiro carbon atom present in the isomers of the present concern makes 5- and 6- mambered rings to be independent of each other in conveying the electronic effects.

Table 7. The λ_{max} values of some of the griseofulvin isomers considered.

Isomers	λ_{max} (nm)
I (Griseofulvin) (*exo*)	279.94, 327.33
II (Griseofulvin) (*endo*)	273.30, 305.45
III (*exo*)	276.34, 329.57
IV (*endo*)	281.37
V (*exo*)	281.45, 336.68
VI (*endo*)	317.05
VII (*exo*)	274.49
VIII (*endo*)	306.39

See Figure 6 for the structures.

4. Conclusion

The present computational study considered some stereo/regio isomers of well known antifungal agent griseofulvin within the restrictions of DFT study at the levels of B3LYP/6-31+G(d) and partly B3LYP/6-31++G(d,p). The present results have indicated that in the vacuum conditions, all the structures are characterized with exothermic heat of formation and favorable Gibbs free energy of formation values and they are electronically stable. Griseofulvin is an effective agent but it possesses some toxic side effects and requires prolong treatment. Within the group of isomers considered there exist some structures having some values which imply quite high resembles to griseofulvin which could be worth studying pharmacologically. The present results may initiate some pharmacological research in the direction of less toxic but more effective alternative agent(s).

References

[1] Egorov, N.S. (1980). *Antibiotics, a scientific approach*. Moscow: Mir Pub.

[2] Sheklakov, N.D., & Milich, M.V. (1974). *Mycoses in man*. Moscow: Mir Pub.

[3] De Carli, L., & Larizza, L. (1988). Griseofulvin. *Mutation Research/Reviews in Genetic Toxicology*, *195*(2), 91-126.

[4] Asger, B., Mads, H.R., Thomas O.L., & Mads, H.C. (2014). The chemistry of griseofulvin. *Chem. Rev.*, *11(*24), 12088-12107. https://doi.org/10.1021/cr400368e

[5] Mustafa, A. (1974). *Chemistry of heterocyclic compounds* (Vol. 29, pp. 370-430). New York: John Wiley and Sons.

[6] Aris, P., Wei, Y., Mohamadzadeh, M., & Xia, X. (2022). Griseofulvin: an updated overview of old and current knowledge. *Molecules*, *27*, 7034. https://doi.org/10.3390/molecules27207034

[7] Oxford, A.E., Raistrick, H., & Simonart, P. (1939). Studies in the biochemistry of micro-organisms: Griseofulvin, $C_{17}H_{17}O_6Cl$, a metabolic product of *Penicillium griseofulvum* Dierckx. *Biochem. J.*, 33, 240-248. https://doi.org/10.1042/bj0330240

[8] Mac Millan, J. J. (1953). Griseofulvin. Part VII. Dechlorogriseofulvin. *Chem. Soc.*, 1697-1702. https://doi.org/10.1039/JR9530001697

[9] Develoux, M. (2001). Griseofulvin. *Annales de dermatologie et de venereologie*, *128*(12), 1317-1325.

[10] Cáceres-Ríos, H., Rueda, M., Ballona, R., & Bustamante, B. (2000). Comparison of terbinafine and griseofulvin in the treatment of tinea capitis. *Journal of the American Academy of Dermatology*, *42*(1), Part 1, 80-84. https://doi.org/10.1016/S0190-9622(00)90013-6

[11] Tey, H.L., Tan, A.S.L., & Chan, Y.C. (2011). Meta-analysis of randomized, controlled trials comparing griseofulvin and terbinafine in the treatment of tinea capitis. *Journal of the American Academy of Dermatology, 64*(4), 663-670. https://doi.org/10.1016/j.jaad.2010.02.048

[12] Aggarwal, N., Goindi, S., & Khurana, R. (2013). Formulation, characterization and evaluation of an optimized microemulsion formulation of griseofulvin for topical application, *Colloids and Surfaces B: Biointerfaces*, *105*, 158-166. https://doi.org/10.1016/j.colsurfb.2013.01.004

[13] Gupta, A.K., Williams, J.V., Zaman, M., & Singh, J. (2009). *In vitro* pharmacodynamic characteristics of griseofulvin against dermatophyte isolates of *Trichophyton tonsurans* from tinea capitis patients. *Medical Mycology*, *47*(8), 796-801. https://doi.org/10.3109/13693780802712523

[14] Zhong, N., Chen, H., Zhao, Q., Wang, H., Yu, X., Eaves, A.M., Sheng, W., Miao, J., Cui, F., & Wang, J. (2010). Effects of griseofulvin on apoptosis through caspase-3- and caspase-9-dependent pathways in K562 leukemia cells: an *in vitro* study. *Current Therapeutic Research, 71*(6), 384-397. https://doi.org/10.1016/S0011-393X(10)80004-9

[15] Bai, Y-B., Gao, Y-Q., Nie, X-D., Tuong, T-M-L., Li, D., & Gao, J-M. (2019). Antifungal activity of griseofulvin derivatives against phytopathogenic fungi *in vitro* and *in vivo* and three-dimensional quantitative structure-activity relationship. *Analysis Journal of Agricultural and Food Chemistry*, *67* (22), 6125-6132. https://doi.org/10.1021/acs.jafc.9b00606

[16] Paguigan, N.D., Al-Huniti, M.H., Raja, H.A., Czarnecki, A., Burdette, J.E., González-Medina, M., Medina-Franco, J.L., Polyak, S.J., Pearce, C.J., Croatt, M.P., & Oberlies, N.H. (2017). Chemoselective fluorination and chemoinformatic analysis of griseofulvin: natural vs fluorinated fungal metabolites. *Bioorganic & Medicinal Chemistry*, *25*(20), 5238-5246. https://doi.org/10.1016/j.bmc.2017.07.041

[17] Mahmoud, W.H., Mahmoud, N.F., & Mohamed, G.G. (2018). Synthesis, characterization, density functional theory, X-ray study, thermal stability, and biological and MOE relevance of metal complexes of griseofulvin. *Applied Organometalic Chemistry*, *32*(5), e4312 . https://doi.org/10.1002/aoc.4312

[18] Knoblauch, J., & Zimmermann, I. (2007). Thermochemical analysis of the dissolution process of Griseofulvin. *European Journal of Pharmaceutics and Biopharmaceutics*, *67*(3), 743-751. https://doi.org/10.1016/j.ejpb.2007.04.012

[19] Lässer, J., & Braun, D.E.(2025). Exploring coformer substitution in cocrystallization: griseofulvin and phenol derivatives. *Crystal Growth & Design*, *25*(5), 1688-1707. https://doi.org/10.1021/acs.cgd.5c00065

[20] Das, S., & Sandip, P. (2016). Computer simulation studies of the mechanism of hydrotrope-assisted solubilization of a sparingly soluble drug molecule. *The Journal of Physical Chemistry B, 120*(14), 3540-3550. https://doi.org/10.1021/acs.jpcb.5b11902

[21] Stewart, J.J.P. (1989). Optimization of parameters for semi-empirical methods I. *J. Comput. Chem.*, *10*, 209-220. https://doi.org/10.1002/jcc.540100208

[22] Stewart, J.J.P. (1989). Optimization of parameters for semi-empirical methods II. *J. Comput. Chem., 10*, 221-264. https://doi.org/10.1002/jcc.540100209

[23] Leach, A.R. (1997). *Molecular modeling*. Essex: Longman.

[24] Kohn, W., & Sham, L.J. (1965). Self-consistent equations including exchange and correlation effects. *Phys. Rev.*, *140*, 1133-1138. https://doi.org/10.1103/PhysRev.140.A1133

[25] Parr, R.G., & Yang, W. (1989). *Density functional theory of atoms and molecules*. London: Oxford University Press.

[26] Becke, A.D. (1988). Density-functional exchange-energy approximation with correct asymptotic behavior. *Phys. Rev. A*, *38*, 3098-3100. https://doi.org/10.1103/PhysRevA.38.3098

[27] Vosko, S.H., Wilk, L., & Nusair, M. (1980). Accurate spin-dependent electron liquid correlation energies for local spin density calculations: a critical analysis. *Can. J. Phys*., *58*, 1200-1211. https://doi.org/10.1139/p80-159

[28] Lee, C., Yang, W., & Parr, R.G. (1988). Development of the Colle-Salvetti correlation energy formula into a functional of the electron density. *Phys. Rev. B*, *37*, 785-789. https://doi.org/10.1103/PhysRevB.37.785

[29] SPARTAN 06 (2006). Wavefunction Inc. Irvine CA, USA.